



## **Influence of Creep on the Stability of Steel Columns Subjected to Fire**

M.A. Morovat<sup>1</sup>, M.D. Engelhardt<sup>2</sup>, T.A Helwig<sup>3</sup>, E.M. Taleff<sup>4</sup>

### **Abstract**

This paper presents highlights of on-going research, which aims at developing analytical, computational and experimental predictions of the phenomenon of creep buckling in steel columns subjected to fire. Analytical solutions using the concept of time-dependent tangent modulus are developed to model time-dependent buckling behavior of steel columns at elevated temperatures. Results from computational creep buckling studies using Abaqus are also presented, and compared with analytical predictions. Material creep data on ASTM A992 steel is also presented in the paper and compared to existing creep models for structural steel. Both analytical and computational methods utilize material creep models for structural steel developed by Harmathy, and by Fields and Fields. Predictions from this study are also compared against those from Eurocode 3 and the AISC Specification. It is clear from results presented in this paper that having an accurate knowledge of material creep is essential in predicting column buckling behavior at elevated temperatures. There is clearly a need for more extensive and reliable creep data for structural steel. Most importantly, results show that neglecting creep effects can lead to significant errors in predicting the strength of steel columns subjected to fire.

### **1. Introduction**

Successful implementation of performance-based structural-fire safety philosophy in designing steel structures depends on accurate predictions of thermal and structural response to fire. An important aspect of such predictions is the ability to evaluate strength of columns at elevated temperatures. Columns are critical structural elements, and failure of columns can lead to collapse of structures. One of the critical factors affecting the strength of steel columns at elevated temperatures is the influence of material creep. Under fire conditions, steel columns can exhibit creep buckling, a phenomenon in which the critical buckling load for a column depends not only on slenderness and temperature, but also on duration of applied load. Although material creep and consequently the phenomenon of creep buckling can significantly impact the safety of steel columns subjected to fire, they have received relatively little research attention, and are not currently explicitly considered in code-based design formula for columns at elevated temperatures, such as those in the Eurocode 3 or in the AISC Specification. This paper presents

---

<sup>1</sup> Graduate Research Assistant, University of Texas at Austin, <morovatma@mail.utexas.edu>

<sup>2</sup> Professor, University of Texas at Austin, <mde@mail.utexas.edu>

<sup>3</sup> Associate Professor, University of Texas at Austin, <thelwig@mail.utexas.edu>

<sup>4</sup> Professor, University of Texas at Austin, <taleff@mail.utexas.edu>

highlights of on-going research on the phenomenon of high-temperature creep buckling of steel columns.

## 2. Creep of Steel at Elevated Temperatures

### 2.1 Background on Creep

It is generally accepted that for ductile materials like steel, plastic strain is a function of shear stress and time at any specific temperature. Therefore, for design purposes, it is usually assumed that the total plastic strain at a constant temperature can be broken into a *time-independent component* or *slip* and a *time-dependent component* or *creep*. For typical loading rates seen in buildings, the inelastic response of steel at room temperature shows a very mild dependence on loading rate and virtually no dependence on time. Therefore, time effects are normally neglected in the analysis and design of steel structures at ambient temperature. However, as temperature increases, steel exhibits increasingly significant creep effects.

Creep tests, either in tension or compression, are usually conducted by subjecting a material to constant load, hence constant engineering stress at a specific temperature, and then measuring engineering strain as a function of time. A typical creep curve is often divided into the three stages of primary, secondary and tertiary creep. In the primary stage, the curve is nonlinear and typically exhibits a decreasing creep strain rate with increase in time. In the secondary stage, the creep strain rate is almost constant, and this stage is often referred to as steady-state creep. In the tertiary stage, the creep strain rate increases with time in an unstable manner. For steel, the shape of the curve, the magnitude of the creep strain and the time scale are greatly affected by both the temperature and the stress level.

Experimental and empirical models have been developed to predict creep strain of steel at elevated temperatures (Norton 1929; Bailey 1929; Zener and Hollomon 1944; Dorn 1955; Harmathy 1967; Fields and Fields 1989). One of the simplest and most widely used creep models is the Norton-Bailey model, also known as the creep power law (Norton 1929; Bailey 1929). It should be noted that although the Norton-Bailey law is capable of modeling primary creep, it can define the steady-state or secondary stage of creep more accurately. One of the widely used creep models in structural-fire engineering applications proposed by Fields and Fields (1989) incorporates a power law and represents creep strain,  $\varepsilon_c$ , in the form of a Norton-Bailey equation as follows:

$$\varepsilon_c = at^b \sigma^c \quad (1)$$

In this equation,  $t$  is time and  $\sigma$  is stress. The parameters  $a$ ,  $b$  and  $c$  are temperature-dependent material properties. Fields and Fields (1989) derived equations for these temperature-dependent material properties for ASTM A36 steel. The model developed by Fields and Fields (1989) is capable of predicting creep in the temperature range of 350 °C to 600 °C and for creep strains up to 6-percent. For initial studies of creep buckling of steel columns at elevated temperatures, one of the creep models used by the authors was the Fields and Fields (1989) model. The application of this creep model together with observations will be discussed in more detail in the following sections of this paper.

Another creep model used by the authors in their study of creep buckling phenomenon at high temperatures is the one developed by Harmathy (1967). Harmathy (1967) appears to be one of the first investigators who attempted at developing creep formula for structural steels at elevated temperatures. Harmathy proposed a creep model based on experiments on several structural and prestressing steels including ASTM A36. His model attempts to predict creep strains in both the primary and secondary stages of creep using the concept of activation energy for creep,  $Q_c$ . The model proposed by Harmathy (1967) represents creep strain,  $\varepsilon_c$ , for steel as follows:

$$\varepsilon_c \approx (3Z\varepsilon_{c_0}^2)^{1/3} \theta^{1/3} + Z\theta \quad \text{when } \frac{d\sigma}{dt} = 0 \quad \text{and } \theta = \int_0^t e^{Q_c/RT} dt \quad (2)$$

In this equation,  $\theta$  is the temperature-compensated time in Dorn's creep theory (Dorn 1955),  $Z$  is the slope of the secondary part of the creep curve ( $\varepsilon_c$  versus  $\theta$ ), also known as the Zener-Hollomon parameter (Zener and Hollomon 1944), and  $\varepsilon_{c_0}$  is the intercept obtained by extending the straight-line section (secondary part) of the  $\varepsilon_c(\theta)$  curve to the  $\varepsilon_c$  axis. The parameters  $\varepsilon_{c_0}$ , and  $Z$  are stress-dependent material parameters.

Although models developed by Fields and Fields (1989) and Harmathy (1967) are referenced by many investigators in the field of structural-fire engineering, their predictions of creep strain for some applied stress levels and temperatures are quite different. As an example, predictions from these two models for ASTM A36 steel are compared and plotted in Fig. 1 for an applied stress of 23 ksi at 500 °C. As can be observed from this plot, the differences in the two models are significant. This difference in creep predictions and its impact on creep buckling behavior will be discussed in the following sections and emphasized throughout this paper.

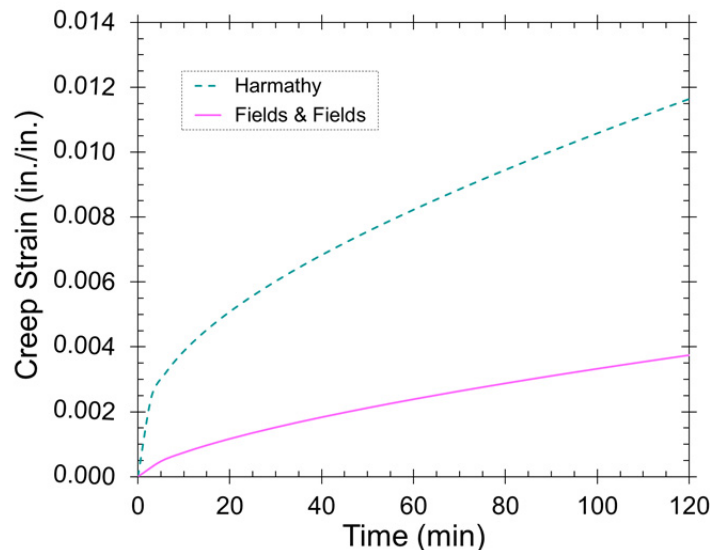


Figure 1: Comparison between Fields and Fields' (1989) and Harmathy's (1967) Models at 23 ksi and 500 °C

## 2.2 Creep of ASTM A992 Steel at Elevated Temperatures

In this section, representative results of a comprehensive material creep investigation of ASTM A992 steel at elevated temperatures are presented and discussed. In addition, these experimental creep results are compared against the creep material models by Fields and Fields (1989) and by

Harmathy (1967) to verify the accuracy and reliability of their predictions. As mentioned in the previous section, creep tests are usually conducted by subjecting the material to constant stress and temperature, and then measuring strain as a function of time. Such tests are commonly referred to as steady state tests, in which the specimens are heated up to a specified temperature and then loaded to the desired stress while maintaining the same temperature. It should be also mentioned that during the initial heating process, the load is maintained at zero to allow free expansion of the specimen. As far as the steel material is concerned, almost all specimens were cut from the web and flanges of a W4×13 section made from ASTM A992 structural steel. Some specimens were also cut from the web of a W30×99 section which is also of ASTM A992 steel.

Representative results of creep tests on ASTM A992 steel are shown in Fig. 2 for materials from the webs of the W4×13 ( $F_y = 60$  ksi) and the W30×99 ( $F_y = 62$  ksi) sections. This figure simply shows the measured creep strain versus time response of ASTM A992 steel after being exposed to specified constant stresses at 500 °C and 700 °C. As can be observed from Fig. 2, it is clear that creep effects are highly significant in the stress-strain response of structural steel at temperatures on the order of 500 °C to 700 °C; temperatures that can be expected in steel members during a fire. It should be specifically noted that some of the curves in Figs. 2(a) and 2(b) show very large creep strains in the time frame of one to two-hours, which may be considered a representative time frame for a compartment fire. Interestingly, curves at 700 °C indicate that the material from the web almost immediately enters the tertiary stage of creep, with a rapid increase in creep strain over a short time interval. In the case of the W4×13 web material, the coupon actually fractured approximately after 44 minutes, a phenomenon known as *stress rupture* or *creep fracture*.

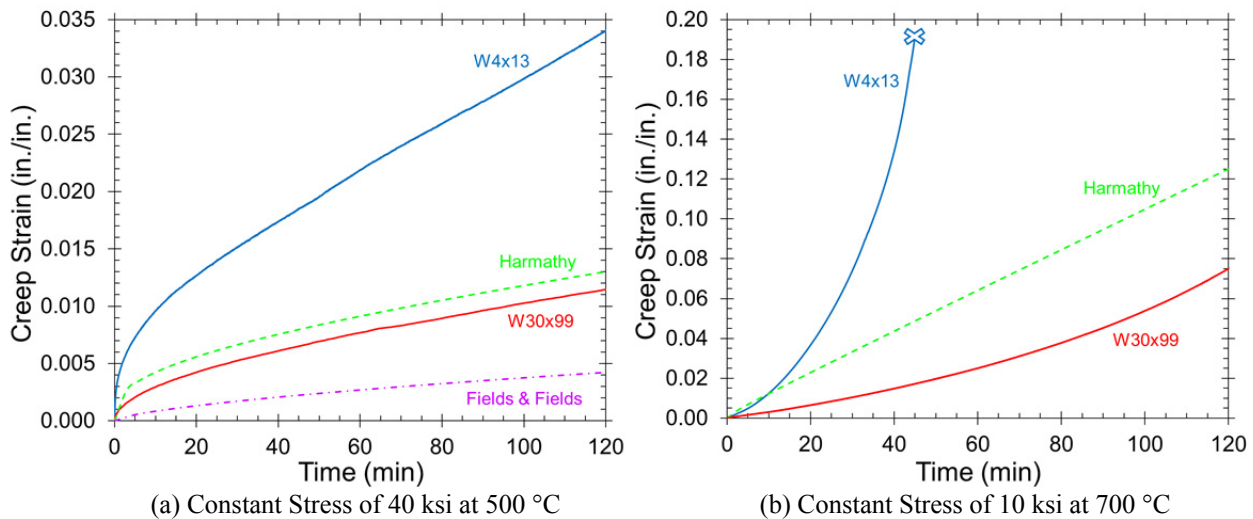


Figure 2: Verification of Material Creep Models against the Web Materials of W4×13 and W30×99

Figs. 2(a) and 2(b) also compare experimental results from the web material of the W4×13 sections and the web material of the W30×99 section. As is clear, there is appreciable difference in material creep response between the two specimens that are both ASTM A992 steel. This observation suggests that there may be large variability in creep response for a particular grade of steel, and this variability should be considered in any attempt at developing *general* material creep models for structural steel at elevated temperatures. Note that some of this variability may

be due to experimental error resulting from factors such as non-uniform temperature distribution over the gage-length of the steel coupons, inaccuracies involved in temperature and strain measurements, inaccuracies in maintaining constant stress, etc.

Predictions from material creep models are also compared with experimental results in Figs. 2(a) and 2(b). As can be seen in these figures, there is not generally a very good agreement between material creep model predictions and experimental creep results. It should be noted that in order to compare the experimental material creep predictions to those from Fields and Fields (1989) and Harmathy (1967) models, corrections must be made due to the difference in materials. As mentioned before, these two material creep models are developed for ASTM A36 steel, not for ASTM A992 steel. A suggested methodology to make this correction is to adjust for the stress values considering the difference in yield strength of materials in consideration (Luecke et al. 2005). Since ASTM A36 steel has lower yield strength than that of ASTM A992 steel, the stress values should be reduced in creep equations (a reduction factor equal to the ratio of 36 ksi to 60 ksi has been considered). Therefore, some of the discrepancies observed in Fig. 2 are due to such stress adjustments. Moreover, in order to draw any conclusion on inconsistencies observed in Fig. 2, limitations in the scope of creep models and approximations involved have to be carefully considered. It should also be added that the creep models by Fields and Fields (1989) and by Harmathy (1967) are suitable for predicting creep strains in the primary and secondary stages of creep. As a result, they cannot capture tertiary creep behaviors observed at 700 °C as can be seen in Fig. 2(b). All in all, observations like these clearly indicate the need for more reliable creep models for structural steel at elevated temperatures.

### **3. Creep Buckling of Steel Columns at Elevated Temperatures**

#### *3.1 Background on Creep Buckling*

The term *creep buckling*, as used herein, refers to the phenomenon in which the critical buckling load for a column depends not only on slenderness and temperature of the column, but also on the duration of applied load. Since creep effects are not significant at room temperature, the buckling load for a steel column of given effective slenderness  $KL/r$  at room temperature is independent of the duration of applied load. As temperature increases, the initial buckling load (at time zero) decreases, due to the decrease in material strength, modulus and proportional limit. Consequently, the buckling capacity at initial application of load depends only on temperature. But, as temperature increases and material creep becomes significant, the buckling load depends not only on temperature, but also on the duration of load application.

#### *3.2 Creep Buckling Analysis of Steel Columns – Analytical Treatment*

To better evaluate the potential importance of creep buckling in structural-fire engineering applications, preliminary creep buckling analyses have been conducted by the authors. These analyses, analytical and computational, attempt to predict the elevated-temperature creep buckling strength of a pin ended steel column. For these analyses, a W12×120 section made of ASTM A36 steel is considered. Moreover, the effective slenderness ratio is kept constant by considering only one single column length of 240 inches.

For the analytical creep buckling studies, the concept of time-dependent tangent modulus proposed by Shanley (1952) is utilized, along with the creep material models developed by Harmathy (1967) and by Fields and Fields (1989), both for ASTM A36 steel. This analytical

method basically uses the Euler buckling equation and replaces Young's Modulus,  $E$ , with the tangent modulus,  $E_T$ , which is a function of time, stress and temperature. In order to calculate the time-dependent tangent modulus, the isochronous stress-strain curves need to be constructed. Simply put, isochronous stress-strain curves are constant-time stress-strain curves derived from creep curves. The slope of the tangent to the isochronous stress-strain curve at any stress and time value is the time-dependent tangent modulus. Since the material creep equation by Fields and Fields (1989) has a simple form, it can be used to explain the procedure of constructing isochronous stress-strain curves and evaluating time-dependent tangent moduli correspondingly. At a specific time, Eq. 1 can be rewritten as follows,

$$\varepsilon_c = a_o \sigma^c \quad (3)$$

where  $a_o$  is equal to  $at^b$  and is constant. In fact, since  $a_o$  is dependent on  $a$ ,  $b$  and  $t$ , it is both temperature and time dependent. It can also be inferred from Eq. 3 that each constant-time, stress-creep strain curve is conceptually equivalent to a time-independent stress-plastic strain curve, here with the power law representation (Morovat et al. 2010). As a result, the total strain which is the sum of elastic, plastic (time-independent inelastic) and creep (time-dependent inelastic) strains can be written as,

$$\varepsilon = \sigma/E + f\sigma^s + a_o \sigma^c \quad (4)$$

Eq. 4 therefore represents the isochronous stress-strain curves based on the creep model by Fields and Fields (1989). Representative isochronous stress-strain curves based on Eq. 4 at 400 °C are shown in Fig. 3.

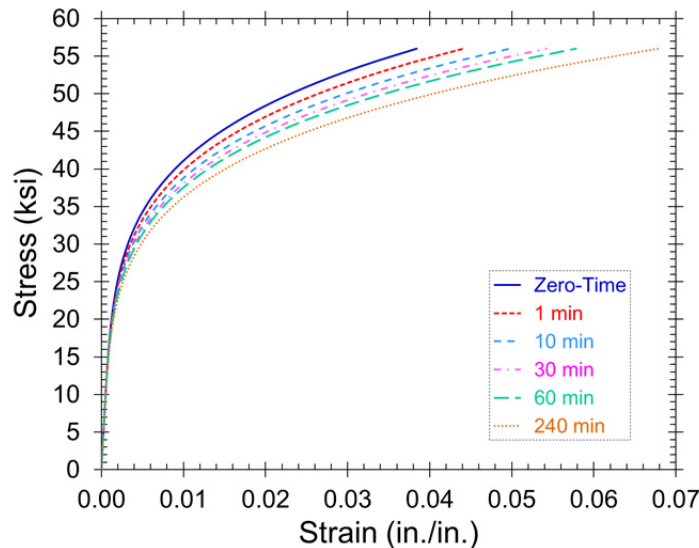


Figure 3: Representative Isochronous Stress-Strain Curves at 400 °C

Eq. 4 can be further used to derive an expression for time-dependent tangent modulus. In other words, using the differential form of Eq. 4. and considering the tangent to be the slope of the

stress-strain curve,  $d\sigma/d\varepsilon$ , a mathematical expression relating tangent modulus to stress can be derived as follows,

$$E_T = \frac{E}{1 + [fg\sigma^{(g-1)} + a_0 c \sigma^{(c-1)}] E} \quad (5)$$

in which,  $E$  is the temperature-dependent Young's modulus and  $E_T$  is the tangent modulus, here a function of both time and temperature. Representative isochronous tangent modulus-stress curves based on Eq. 5 at 400 °C are shown in Fig. 4.

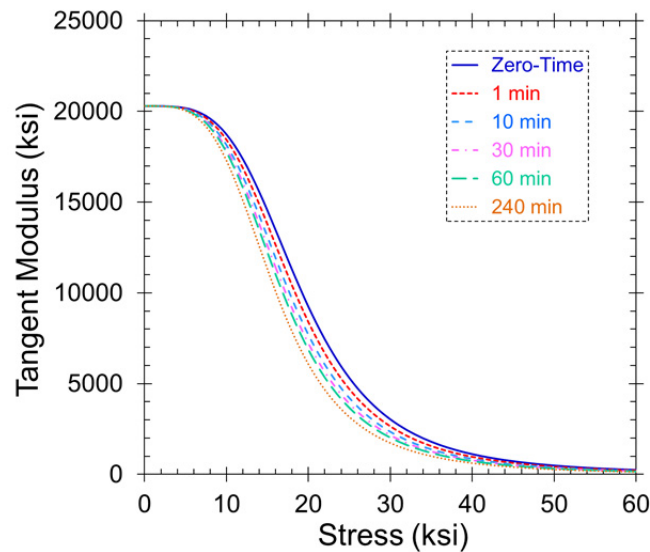


Figure 4: Representative Isochronous Tangent Modulus-Stress Curves at 400 °C

Isochronous tangent modulus-stress curves constructed using Eq. 5 can be used to determine creep buckling loads graphically. From the classical tangent modulus theory for inelastic column behavior, the relationship between stress and tangent modulus at a specific temperature can be written as,

$$\sigma = \frac{\pi^2 E_T}{(KL/r)} \quad \text{or} \quad E_T = \frac{(KL/r)^2}{\pi^2} \sigma \quad (6)$$

From Eq. 6, it can be deduced that constant slenderness ratios represent straight lines through the origin on the tangent modulus-stress plots. Intersections of such lines with each tangent modulus-stress isochrone have horizontal components on the stress axis. These stress components are therefore time-dependent buckling stresses for the column in consideration. In addition, the time isochrone corresponding to each specific creep stress and consequently the creep buckling load is referred to as the failure time or time-to-buckle.

The process of graphical evaluation of creep buckling stresses is further illustrated in Fig. 5, where two straight lines associated with two different slenderness ratios for a W12×120 column

are shown along with isochronous tangent modulus-stress curves determined using Eq. 5 at 500 °C. As an example, for the failure time of 240 minutes in Fig. 5, the creep buckling stress of about 11.8 ksi (creep buckling load of 414 kips) is predicted for the column length of 240 inches.

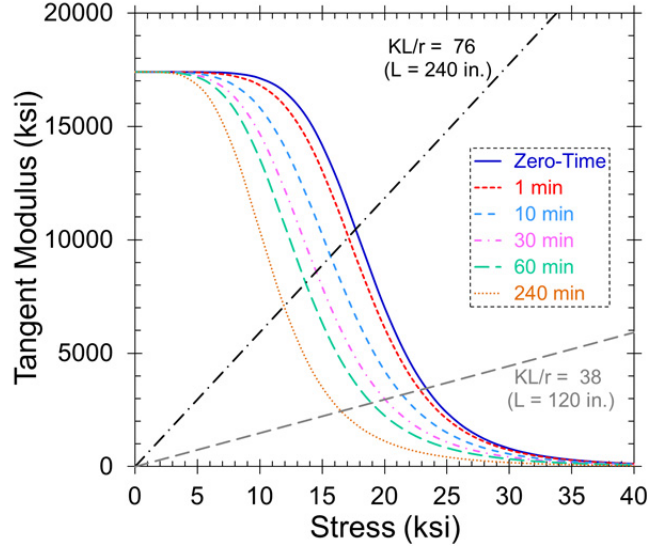


Figure 5: Graphical Representation of the Concept of Creep Buckling at 500 °C

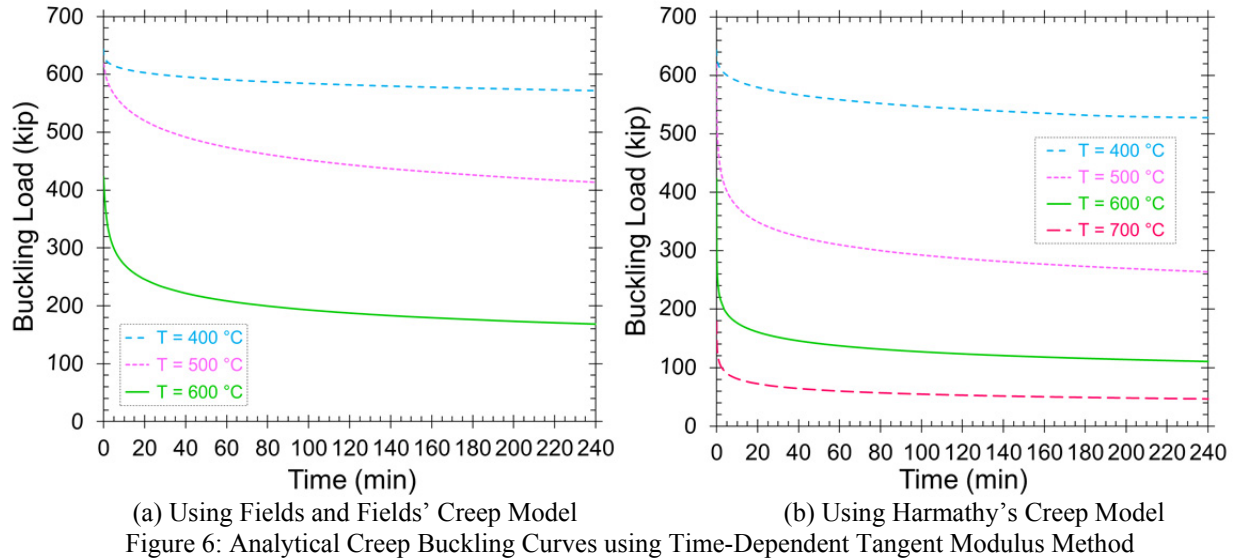
In addition to the graphical solution described above, Eq. 5 can be used to obtain creep buckling curves numerically. Since  $E_T/E = P_{cr}/P_E$ , Eq. 5 yields an equation for creep buckling, which is shown as Eq. 7.

$$P_{cr} = \frac{P_E}{1 + [fg\sigma^{(g-1)} + a_0c\sigma^{(c-1)}]E} \quad (7)$$

$P_E$  is the Euler buckling load at elevated temperatures in Eq. 7. At buckling,  $\sigma = \sigma_{cr} = P_{cr}/A$ , therefore Eq. 7 can be rewritten as follows,

$$P_{cr} + \left[ \frac{fgE}{A^{(g-1)}} \right] P_{cr}^g + \left[ \frac{a_0cE}{A^{(c-1)}} \right] P_{cr}^c = P_E \quad (8)$$

in which  $A$  is the cross sectional area of the column. Eq. 8 can be solved iteratively to get the  $P_{cr}$  as a function of time at a constant temperature. Sample solutions of Eq. 8 applied to a 240-inch long, W12×120 column are plotted in Fig. 6.



As a final note on the analytical formulation, it should be added that this method disregards any initial imperfections and assumes a perfectly straight column.

### 3.3 Creep Buckling Analysis of Steel Columns – Computational Treatment

As a next step, computational predictions of creep buckling are developed using Abaqus. In order to simulate creep buckling in Abaqus, first, temperature is increased to the desired level, and then a fraction of the zero-time buckling load is applied to the column. No material creep is considered in these two steps. Next, the column is allowed to creep over the time period of 50 hours under the sustained load. Finally, the time-to-buckle due to creep is estimated. It should be pointed out here that to get the zero-time buckling load, an inelastic load-deflection analysis has to be performed. This has been done in Abaqus by using a nonlinear analysis scheme called Riks Analysis. Moreover, to model initial geometric imperfections, an Eigen-value buckling analysis is performed. The initial shape of the column is taken as the shape of the first buckling mode, and the magnitude of the imperfection is chosen as a fraction of the column length. As far as material modeling is concerned, the inelastic material models (both time-independent and creep) at elevated temperatures are defined using the models developed by Fields and Fields (1989) based on material tests by Skinner (1972), explained in the previous section. 3D hexahedral eight-node linear brick elements, *C3D8R*, have been utilized to model the columns in Abaqus.

As an example, the results of creep buckling simulations for the temperature of 500 °C and an initial out-of-straightness of  $L/1000$  are presented in Fig. 7 as plots of creep deflection versus time at different load levels. Fig. 7 clearly shows that the rate of change of deflection with time increases very slowly at the beginning and then increases more rapidly until the column no longer can support its load. The time at which the displacement-time curves become nearly vertical is taken as the *failure time* or *time-to-buckle* in this study.

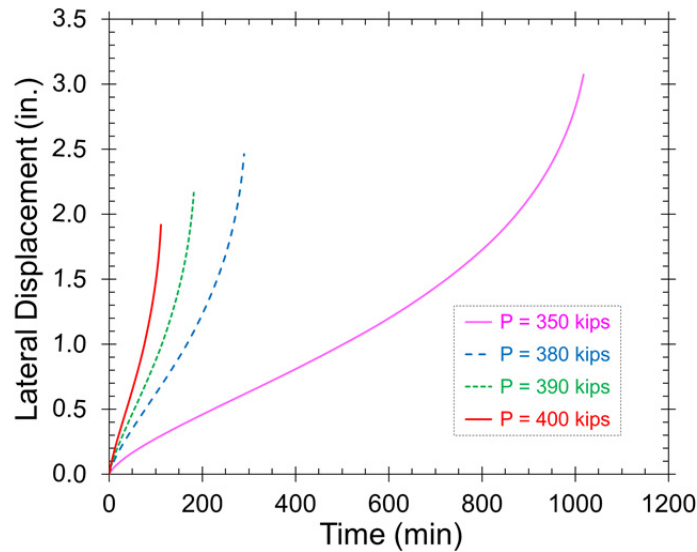


Figure 7: Lateral Deflections due to Creep at 500 °C and  $\Delta_0 = L/1000$

Curves like the ones presented in Fig. 7 can be used to construct time-dependent column buckling curves, examples of which are shown in Fig. 8 for three different temperatures.

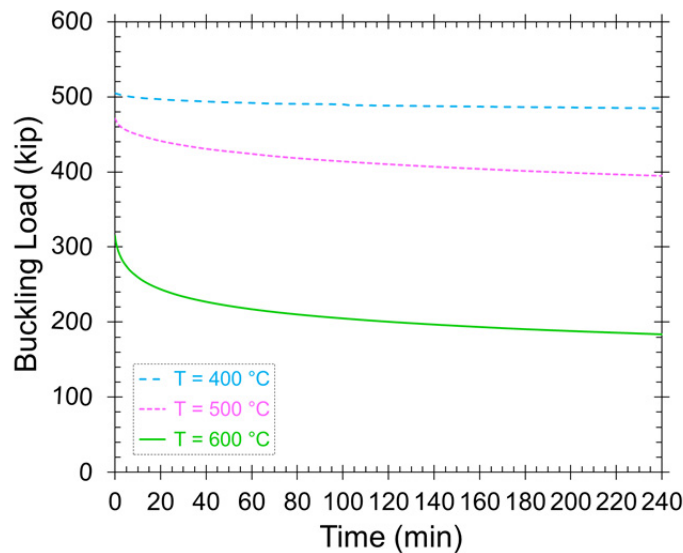


Figure 8: Computational Creep Buckling Curves with  $\Delta_0 = L/1000 = 0.240$  in.

### 3.4 Creep Buckling Analysis of Steel Columns – Analytical versus Computational Predictions

Creep buckling predictions from analytical and computational methods are compared at 600 °C and presented in Fig. 9. The analytical predictions are for a perfect column, while the computational one is for a column with  $L/1000$  initial crookedness. As can be seen in Fig. 9, there is a distinct difference between the zero-time buckling capacity predicted by the computational approach and those predicted by the time-dependent tangent modulus theory even in the cases using the same material creep model proposed by Fields and Fields (1989). The zero-time buckling predictions by the tangent modulus are in fact on the unconservative side.

Unconservative predictions of buckling strength by the tangent modulus theory compared with experiments have been also observed and reported in the literature for columns made of aluminum and titanium alloys with slenderness ratios in the range of about 60 to 80 (Wang 1948; Carlson and Manning 1958). The authors are continuing work to better explain the discrepancy between theoretical buckling predictions using tangent modulus theory versus computational predictions using Abaqus. The explanation, in part, may relate to a very high degree of sensitivity of buckling capacity to initial geometric imperfection for materials with highly nonlinear stress-strain curves, as is the case with structural steel at elevated temperatures. Further discussion is provided below.

In addition to discrepancies in the zero-time buckling load predictions, the differences in theoretical creep buckling predictions observed in Fig. 9 can be related to the difference in predictions of the material creep models by Harmathy (1967) and Fields and Fields (1989), especially in primary creep considerations at high levels of stress as shown in Fig. 1.

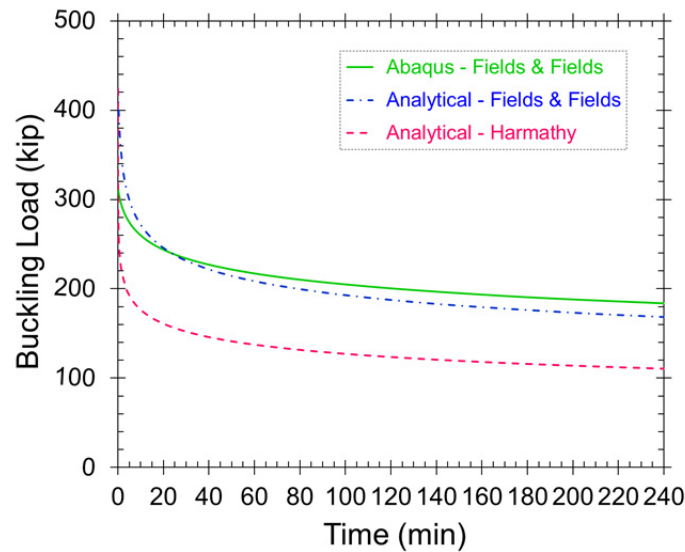


Figure 9: Comparison between Analytical and Computational Creep Buckling Predictions at 600 °C

Creep buckling curves presented in Fig. 9 further suggest a close relationship between the zero-time or time-independent buckling load predictions and the overall creep buckling behavior of steel columns at elevated temperatures due to fire.

As noted above, there appears to be a strong correlation between initial geometric imperfection and the zero-time buckling load predictions at high temperatures. This is further verified in Table 1, where zero-time buckling load predictions using Abaqus and considering different initial imperfections are compared against those predicted by the tangent modulus theory at different temperatures. As can be observed in Table 1, as the magnitude of initial imperfection approaches zero, a better agreement can be reached between time-independent buckling capacities calculated by the theory and simulations. But even for very small deviations from straightness, significant reductions in column buckling capacities can be seen, especially for practical imperfection values in the order of  $L/1000$ , equal to 0.240 in. for the column in consideration. As seen from the data in Table 1 the reduction in buckling strength is very large.

Table 1: Zero-Time Buckling Load Predictions at Elevated Temperatures

Temperature (°C)	$P_{cr}$ (kip)							
	Tangent Modulus	Initial Imperfection Amplitude, $\Delta_o$ (in.)						
		0.010	0.080	0.096	0.120	0.160	0.240	0.480
400	643	615	546	541	534	520	505	472
500	619	603	512	507	500	490	471	433
600	424	419	341	338	333	326	315	291

By comparing the zero-time buckling load predictions at different temperatures, it can also be inferred that the highly nonlinear stress-strain behavior of structural steel at elevated temperatures like 400 and 500 °C, has an amplifying effect on the role of initial geometric imperfection in lowering the load-carrying capacity of steel columns at elevated temperatures. The interactions between nonlinear material behavior and initial crookedness and the resulting impact on steel column strength at high temperatures is an area that definitely deserves more research attention.

The importance of initial geometric imperfections in predicting creep buckling behavior of steel columns at elevated temperatures will be more elaborated in the following section of this paper.

### 3.5 Effect of Initial Geometric Imperfections on Creep Buckling Predictions

Although classical buckling theories are developed on the assumption of perfect columns, imperfections in the form of initial curvatures and load eccentricities always exist in real columns. In fact, initial geometric imperfections have been one of the main sources of discrepancies between theoretical and experimental predictions of column buckling strengths at ambient temperature. Their strong influence on reducing column buckling capacity is well understood and accounted for in modern design codes (Southwell 1932; Timoshenko 1936; Shanley 1947; Ziemian 2010; AISC 2010). As for the role of initial crookedness in elevated-temperature instabilities, while there are published data in the literature suggesting their importance in predicting the buckling strength of steel columns, their influence in the creep buckling analysis is not well established. Therefore, the goal in this section is to provide some insight on how initial geometric imperfections affect creep buckling behaviors through computational column buckling studies using Abaqus.

Figure 10 shows the results of a series of Abaqus simulations of creep buckling tests on 240-inch long, W12×120 steel columns with different initial out-of-straightness at 500 °C. As it is clear from Fig. 10, initial geometric imperfections have major impact on the zero-time or time-independent buckling load predictions, which in turn result in different creep buckling behaviors. More specifically, Fig. 10 indicates that higher initial crookedness values result in lower zero-time buckling capacities of the steel column in consideration at 500 °C. Fig. 10, however, does not clearly show how the initial imperfections affect the creep buckling capacities.

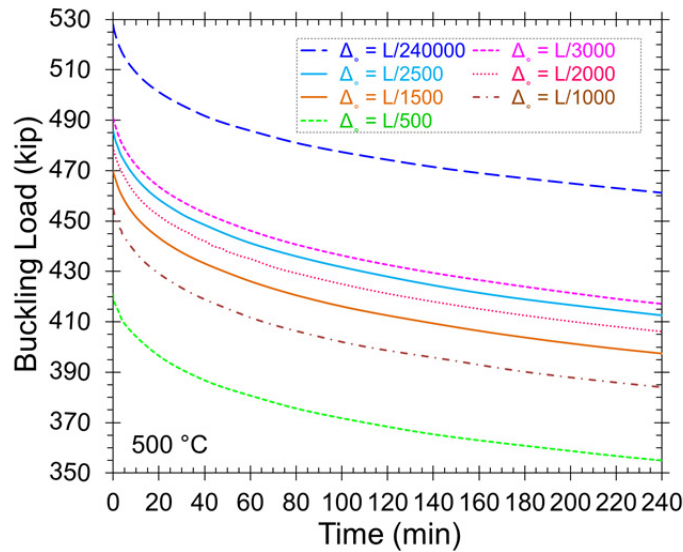


Figure 10: Computational Creep Buckling Predictions Corresponding to Different Initial Imperfections at 500 °C

An instructive way to study the effect of initial out-of-straightness on creep buckling strength of steel columns at elevated temperatures is to construct curves of creep buckling time vs. initial imperfection magnitude for a given column load. Two samples of such curves are presented in Fig. 11 corresponding to sustained loads of 420 and 410 kips. As can be seen from Fig. 11, the creep buckling time drops significantly as the applied load approaches the zero-time buckling load for a specific initial crookedness. In other words, initial imperfections can have a profound impact on creep buckling time of steel columns with low to moderate imperfections, typical of imperfections expected in structural steel columns. For example, in the case of a steel column with an initial imperfection of 0.240 inches, increasing the applied load from 410 to 420 kips reduces the creep buckling time of the column from 121 to 73 minutes.

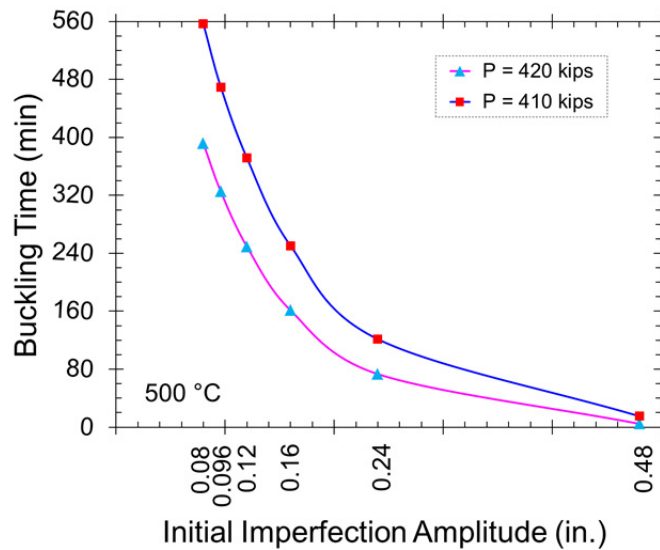


Figure 11: Representative Creep Buckling Time vs. Maximum Initial Imperfection Curves at 500 °C

### 3.6 Effect of Residual Stresses on Creep Buckling Predictions

Residual stresses have been shown to significantly influence the buckling of columns of intermediate slenderness at ambient temperature. Numerous measurements of the magnitude and distribution of residual stresses in rolled and welded steel shapes are available, and their influence on column strength is well understood (Ziemian 2010). However, little is known regarding the influence of magnitude and distribution of residual stresses on column strength at high temperatures.

In this section, an attempt has been made to investigate the importance of residual stresses on creep buckling predictions for steel columns at elevated temperatures. The residual stress pattern suggested by Galambos and Ketter (1959) and Ketter (1960), as shown in Fig. 12, has been used as the room-temperature, initial stress state in computational creep buckling analyses using Abaqus.

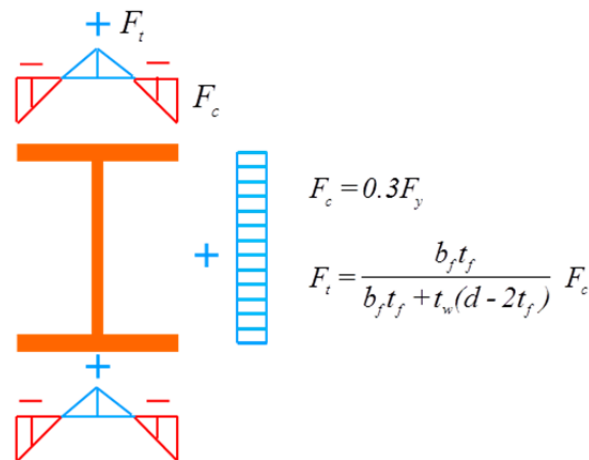


Figure 12: Lehigh Residual Stress Distribution (Galambos and Ketter 1959; Ketter 1961)

The influence of residual stresses on creep buckling predictions at high temperatures is shown in Fig. 13. Curves shown in Fig. 13 are generated as a result of creep buckling simulations on 240-inch long, W12×120 steel columns with the initial imperfection amplitude of  $L/1000$ . As can be observed from Fig. 13, the presence of residual stresses has moderate effects on reducing the zero-time buckling capacities at elevated temperatures even though the apparent effect of differences in zero-time buckling strength predictions upon creep buckling behavior is not clear. It can also be seen from Fig. 13 that the effect of residual stresses on the creep buckling behavior of steel columns becomes less significant at higher temperatures like 600 °C. This may be explained by the fact that at very high temperatures like 600 °C, the material stress-strain response becomes intrinsically highly nonlinear with a significantly reduced proportional limit and the residual stresses have also been relaxed due to the effects of high temperatures.

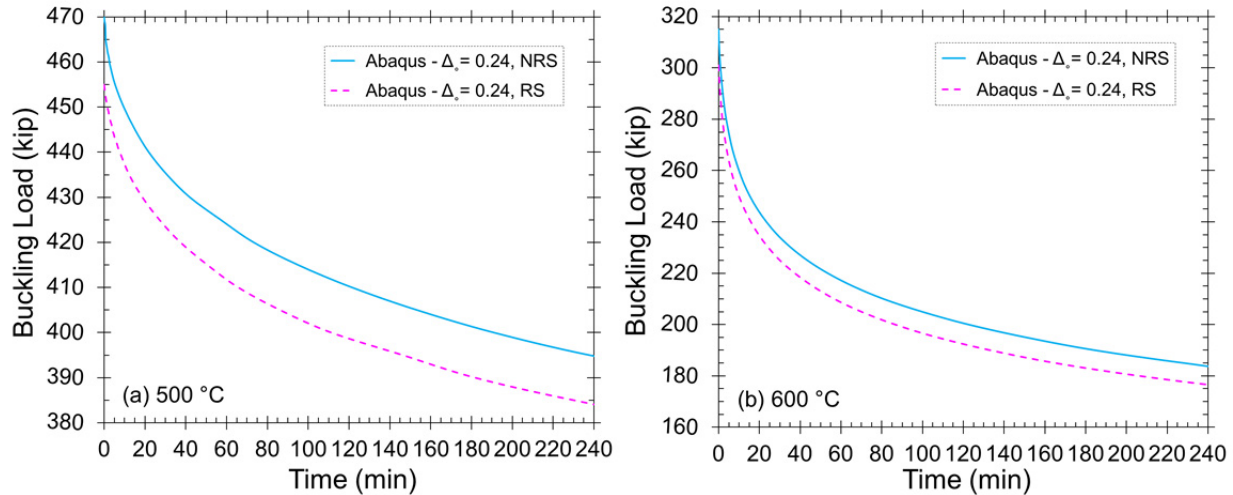


Figure 13: The Effect of Residual Stresses on Creep Buckling Predictions

The effect of residual stresses on creep buckling strength of steel columns at elevated temperatures can also be represented utilizing curves of creep buckling time vs. initial imperfection magnitude at constant column loads. Fig. 14, for instance, plots such curves for a constant load of 420 kips in the presence and absence of residual stresses. It is apparent from curves in Fig. 14 that residual stresses have the most impact on creep buckling capacities of steel columns with low to moderate initial imperfections.

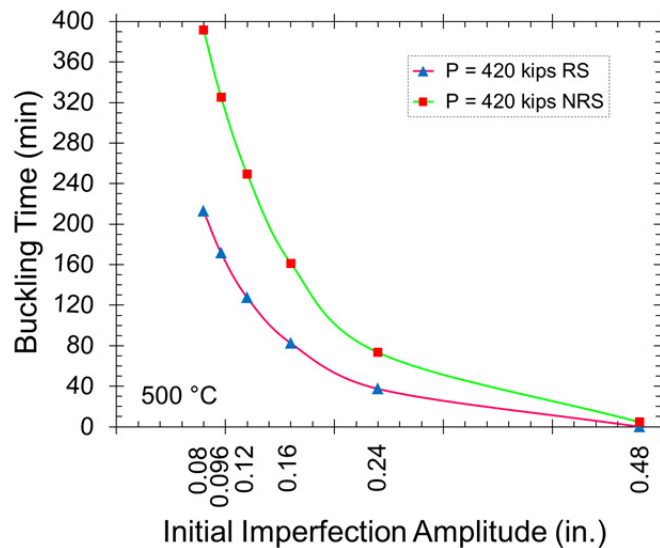


Figure 14: Representative Creep Buckling Time vs. Maximum Initial Imperfection Curves at 500 °C

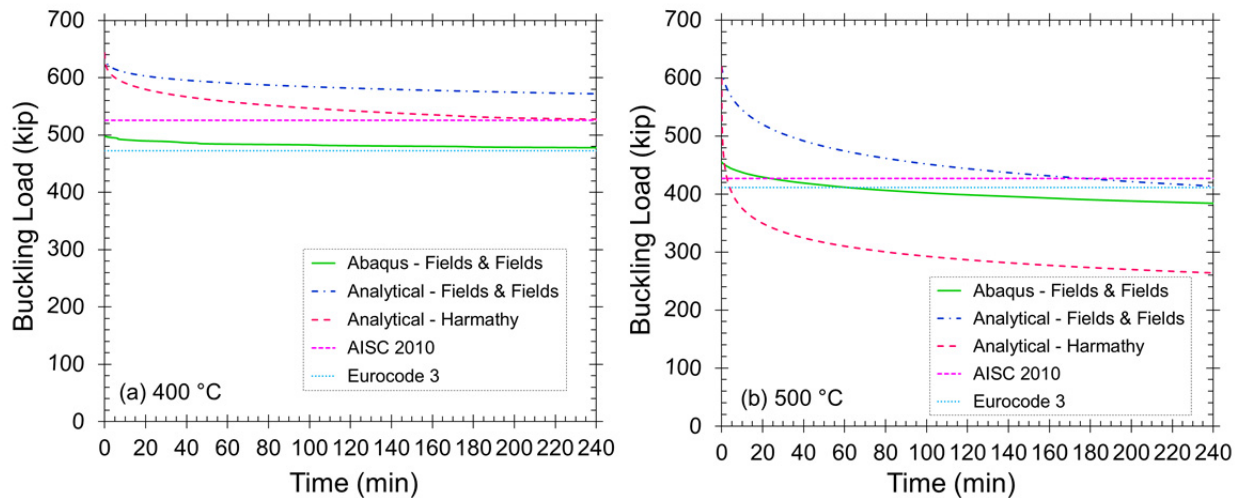
#### 4. Comparison with AISC and Eurocode 3 Predictions

In this section results obtained from analytical and computational creep buckling analyses presented in the previous sections will be compared with the corresponding elevated temperature column strength predictions of AISC (2010) and Eurocode 3 (2006).

It should be pointed out here that formula to predict column strength at high temperatures in Appendix 4 of the 2010 edition of the *AISC Specification for Structural Steel Buildings* are based

on work by Takagi and Deierlein (2007). Both the Eurocode 3 (2006) column strength formula and that proposed by Takagi and Deierlein (2007) predict column strength as a function of temperature, but do not consider duration of load and temperature exposure; i.e., they do not consider creep buckling effects. These formulas are based on computational studies using elevated-temperature stress-strain curves for steel that do not explicitly include creep effects, and are verified against high-temperature column buckling experiments that also did not explicitly consider time dependent effects on buckling.

Fig. 15 depicts the comparison of creep buckling predictions from Abaqus and time-dependent tangent modulus with the ones from Eurocode 3 (2006) and AISC (2010), for a 240-inch long W12×120 column of ASTM A36 steel. Generally speaking, it can be observed that code-based predictions underestimate buckling strength of this column for relatively short load durations, at higher temperatures such as 600 and 700 °C. The problem with code-based predictions of buckling becomes more evident when analytical creep buckling predictions using Harmathy’s material creep model are compared against code-based ones, as shown in Figs. 15(b), 15(c) and 15(d). It is also interesting to note that as temperatures get higher, analytical and computational buckling predictions using the Fields and Fields material creep model get closer, suggesting that the effect of creep is perhaps more important in overall inelastic buckling behavior at higher temperatures. Observations like these clearly show the significance of the need for more reliable creep data for structural steel.



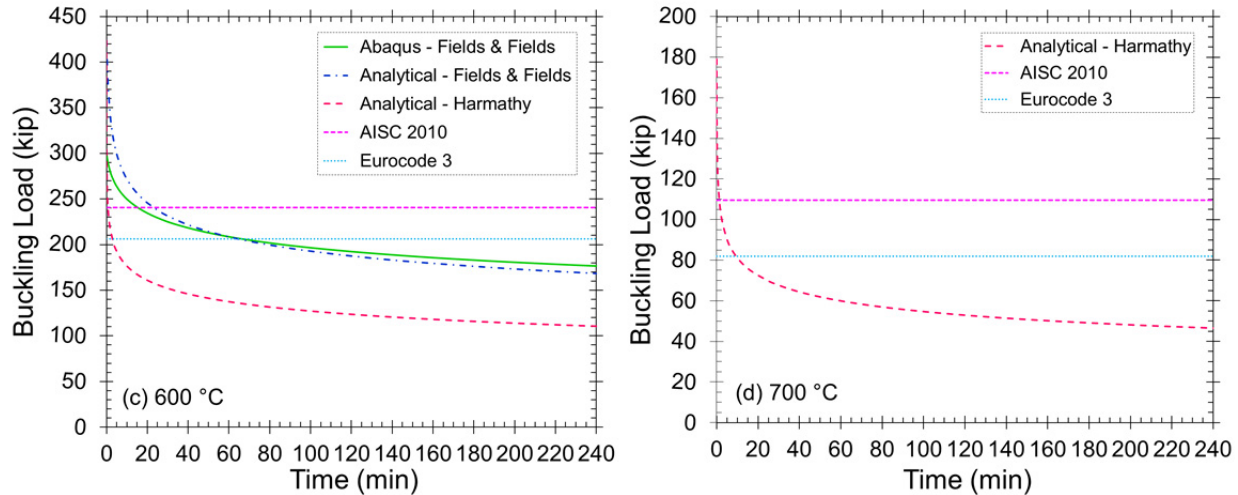


Figure 15: Comparison between Computational and Analytical Creep Buckling Predictions with Code-Based Buckling Predictions

## 5. Conclusion

This paper has presented some results of on-going research on the time-dependent buckling behavior of steel columns subjected to fire. Studies were conducted using a 3D finite element model incorporating both geometric and material nonlinearities. Analytical solutions were also developed to consider material creep effects on the overall time-dependent buckling. Predictions from this study were also compared against those from Eurocode 3 and the AISC Specification.

It is clear from results presented in this paper that material creep is significant within the time, temperature, and stress regimes expected in a building fire and that having an accurate knowledge of material creep is essential in predicting column buckling behavior at elevated temperatures. There is clearly a need for more extensive and reliable creep data for structural steel. In addition, results show that neglecting creep effects can lead to erroneous and potentially unsafe predictions of the strength of steel columns subjected to fire.

## Acknowledgments

The research reported herein was conducted as part of research projects on *Elevated Temperature Performance of Beam End Framing Connections*, on *Creep Buckling of Steel Columns Subjected to Fire* and on *Elevated Temperature Performance of Shear Connectors for Composite Beams*, all supported by the National Science Foundation (NSF Awards 0700682, 0927819 and 1031099, respectively). Elevated temperature material tests were conducted using equipment procured through an NSF Major Research Instrumentation Grant (NSF Award No. CMS-0521086 – *Acquisition of a High-Temperature Testing Facility for Structural Components and Materials*). The support of the National Science Foundation and of the former NSF Program Directors M.P. Singh and Douglas Foutch is gratefully acknowledged. The authors are also grateful to Gerdau-Ameristeel for donating materials for this research. The authors would especially like to thank Matthew Gomez of Gerdau-Ameristeel for his support of this research. Any opinions, findings, and conclusions or recommendations expressed in this paper are those of the authors and do not necessarily reflect the views of the National Science Foundation.

## References

- American Institute of Steel Construction (AISC). (2010). *Specification for Structural Steel Buildings*, Standard ANSI/AISC 360-10, Chicago.
- Bailey, R.W. (1929). "Creep of Steel under Simple and Compound Stress." *Engineering*, 148, 121, 528-529.
- Carlson, R.L., and Manning, G.K. (1957). *A Summary of Compressive-Creep Characteristics of Metal Columns at Elevated Temperatures*, WADC Technical Report 57-96, Contract No. AF33(616)-3317, WADC and Battelle Memorial Institute, April 1957.
- Dorn, J.E. (1955). "Some Fundamental Experiments on High Temperature Creep." *Journal of the Mechanics and Physics of Solids*, 3(2) 85-116.
- Eurocode 3 (2006). *Design of Steel Structures. Part 1-2: General rules. Structural Fire Design*, EN 1993-1-2 European Committee for Standardization, CEN.
- Fields, B.A., and Fields, R.J. (1989). *Elevated Temperature Deformation of Structural Steel*, Report NISTIR 88-3899, NIST, Gaithersburg, MD.
- Galambos, T.V., and Ketter, R.L. (1959). "Columns Under Combined Bending and Trust." *Journal of the Engineering Mechanics Division, ASCE*, 85(EM2) 1-30.
- Harmathy, T.Z. (1967). "A Comprehensive Creep Model." *Journal of Basic Engineering, Trans. ASME*, 89(3) 496-502.
- Ketter, R.L. (1961). "Further Studies on the Strength of Beam-Columns." *Journal of the Structural Division, ASCE*, 87(ST6) 135-152.
- Luecke, W.E. et al. (2005). *Federal Building and Fire Safety Investigation of the World Trade Center Disaster – Mechanical Properties of Structural Steels (Draft)*, Report NIST NCSTAR 1-3D, National Institute of Standards and Technology, Gaithersburg, MD.
- Morovat, M.A., Lee, J., Hu, G., and Engelhardt, M.D. (2010). "Tangent Modulus of ASTM A992 Steel at Elevated Temperatures." *Structures in Fire – Proceedings of the Sixth International Conference*, East Lansing, June 2-4.
- Norton, F.H. (1929). *The Creep of Steel at High Temperatures*, McGraw-Hill Book Company, Inc., New York.
- Shanley, F.R. (1947). "Inelastic Column Theory." *Journal of the Aeronautical Sciences*, 14(5) 261-267.
- Shanley, F.R. (1952). *Weight-Strength Analysis of Aircraft Structures*, McGraw-Hill Book Company, Inc., New York.
- Skinner, D.H. (1972). "Determination of High Temperature Properties of Steel." *Broken Hill Proprietary Company, Technical Bulletin*, 16(2) 10-21.
- Southwell, R.V. (1932). "On the Analysis of Experimental Observations in Problems of Elastic Stability." *Proceedings of the Royal Society of London, Series A*, 135(4) 601-616.
- Takagi, J., and Deierlein, G.G. (2007). "Strength Design Criteria for Steel Members at Elevated Temperatures." *Journal of Constructional Steel Research*, 63 1036-1050.
- Timoshenko, S.P. (1936). *Theory of Elastic Stability*, McGraw-Hill Book Company, Inc., New York.
- Wang, C.T. (1948). "Inelastic Column Theories and an Analysis of Experimental Observations." *Journal of the Aeronautical Sciences*, 15(5) 283-292.
- Zener, C., and Hollomon, J.H. (1944). "Effect of Strain Rate on the Plastic Flow of Steel." *Journal of Applied Physics*, 15 22-32.
- Ziemian, R.D. Editor (2010) *Guide to Stability Design Criteria for Metal Structures*, 6<sup>th</sup> Edition, John Wiley & Sons, Inc., New York.